INFLUENCE OF TRANSVERSE MOTION ON LONGITUDINAL SPACE CHARGE IN THE CERN PS

A. Laut*, A. Lasheen, CERN, Geneva, Switzerland

Abstract

Particles in an intense bunch experience longitudinal self-fields due to space charge. This effect, conveniently described by geometric factors dependent on a particle's transverse position, beam size, and beam pipe aperture, is usually incorporated into longitudinal particle tracking on a per-turn basis. The influence of transverse betatron motion on longitudinal space charge forces is, however, usually neglected in pure longitudinal tracking codes. A dedicated tracking code was developed to characterize the CERN PS such that an effective geometric factor of a given particle could be derived from its transverse emittance, betatron phase advance, and momentum spread. The effective geometry factor is then estimated per particle by interpolation without the need for full transverse tracking and incorporated into the longitudinal tracker BLonD. The paper evaluates this effect under conditions representative of the PS, where space charge is dominant at low energy and progressively becomes negligible along the acceleration ramp. The synchrotron frequency distribution is modified and the filamentation rate is moreover increased, which could suggest a stabilizing space charge phenomenon.

INTRODUCTION

In the Proton Synchrotron (PS) at CERN, longitudinal space charge, defined in Eq. (1) as a beam coupling impedance, dominates other impedance sources at injection where protons are accelerated from a mildly relativist kinetic energy of $E_k = 2$ GeV to a highly relativistic $E_k = 26$ GeV. Proportional to the vacuum impedance Z_0, a geometry factor g, and inversely proportional with $\beta\gamma^2$ [1].

$$\frac{Z}{n} = -j\frac{Z_0}{\beta\gamma^2}g \qquad (1)$$

The space charge geometry factor g describes the longitudinal self fields based on the beam size and aperture [2]. For a particle within a long round beam of uniform transverse density, the geometry factor is often expressed by

$$g = \frac{1}{2} + \ln\frac{b}{a} - \frac{1}{2}\frac{r^2}{a^2}, \qquad (2)$$

where a describes the beam radius, b describes the radius of a conductive aperture, and r describes the particle's radial offset.

Throughout the PS, longitudinal space charge impedance and other purely reactive impedance sources with constant Z/n induce wakefield voltages V_W given by Eq. (3

$$V_W = -\frac{i}{\omega_s}\frac{Z}{n}\frac{d\lambda}{d\tau}, \qquad (3)$$

---

* alexander.laut@cern.ch

where $n = f/f_s$, f_s being the revolution frequency of the synchronous particle, the time coordinate $\tau = t - t_s$ being relative to the synchronous particle, and $d\lambda/d\tau$ being the derivative of $\lambda(\tau)$ the longitudinal bunch profile. Because of the large range of longitudinal space charge observed in the PS throughout the acceleration ramp (Fig.1), the induced wakefield voltage will have a strong and varying influence on the longitudinal dynamics, potentially influencing longitudinal beam stability [3]. To reproduce these effects in simulation, it is important to accurately model space charge in the PS.
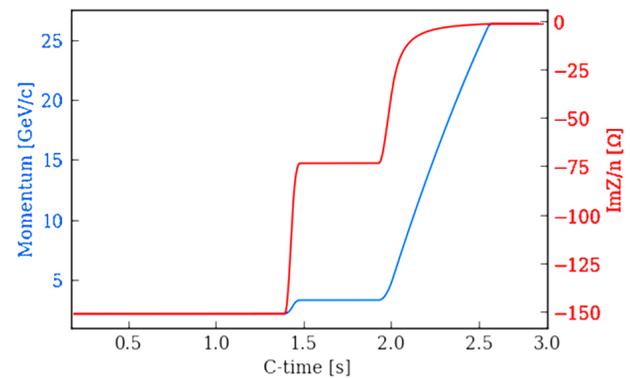

Figure 1: Space charge impedance ImZ/n in the PS which dominates until it is compensated at higher momentum by the inductive impedance of the PS aperture of about 20 Ω [4].

The LHC Injectors Upgrade (LIU) project at CERN [5,6] aims to increase the total intensity of the injectors for both proton and ion beams to reach the requirements for High-Luminosity LHC (HL-LHC) [7]. At flat bottom where particle energies are lower, beam brightness is limited by space charge effects. In the transverse plane, charges within a bunch will repel each other, limiting the minimum transverse emittance. In the longitudinal plane, the self-fields of a bunch will be defocusing below transition energy, and focusing above. As a pure reactive impedance, longitudinal space charge will also influence Landau damping and overall beam stability.

As illustrated in Fig. 2, a bunch can spontaneously break up shortly after transition crossing due to high frequency impedance sources. Longitudinal space charge being a focusing force after transition, and being a function of $d\lambda/d\tau$, will amplify the modulation induced by wakefields.
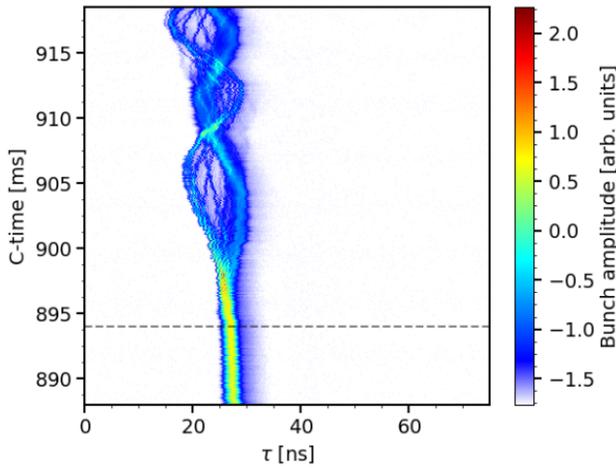
MOP13

Figure 2: Micro-Bunch Instabilities occurring in protons after crossing transition in the PS.

The instability described above was studied using the tracking code BLonD [8], benchmarked first in comparison with a stable bunch. Modeling space charge as an impedance accurately reproduces the bunch oscillations after transition crossing as seen in Fig. 3. However, the predicted space charge impedance must be reduced by 30% to match the oscillation amplitude as observed in experiment [9].
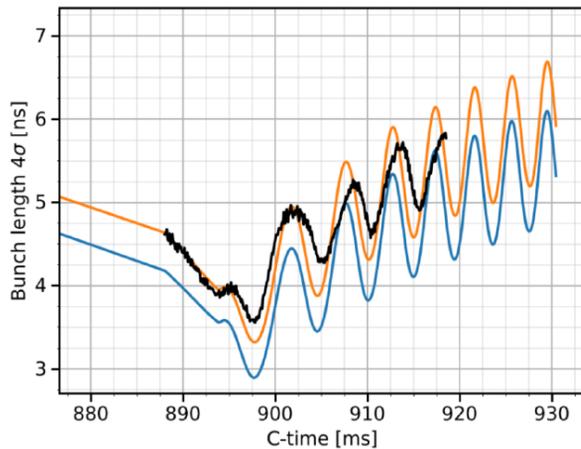

Figure 3: Validation of BLonD space charge model with bunch length oscillations after transition. Reducing impact of space charge by 30% in simulation (blue) improves the match with experimental measurements (black). Bunch lengthening due to the acquisition system's transfer function is simulated in orange.

Another key parameter for longitudinal space charge is the bunch length. For the LHC-type beam in the PS, the beam undergoes a sequence of RF manipulations including batch compression, merging and splitting (the corresponding momentum and RF during the cycle are shown in Fig. 4), leading to an important variation in bunch length of almost two orders of magnitude from injection to extraction. This also translates into a momentum spread which, through dis-

persion, will influence the transverse beam size, which is relevant for studies.
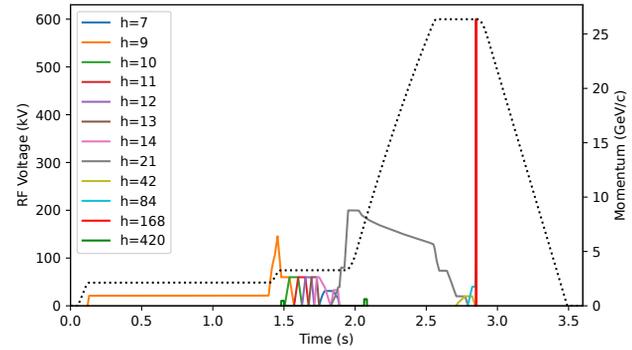

Figure 4: Voltage programs at RF harmonics h and particle momentum are plotted against time during a cycle in the PS.

Conventional longitudinal tracking codes neglect the radial dependency of the geometry factor g by assuming all particles are traveling along the center of the beam where space charge is strongest. Realistically, particles with large transverse emittance or momentum spread will have betatron trajectories further from the center of the beam and experience, on average, less space charge. This is also a particularly poor approximation during transition crossing where momentum spread is high. Naturally, the effects of transverse motion on longitudinal space charge are of key interest for describing the current discrepancy observed between simulation and experiment.

SYNCHROTRON FREQUENCY SHIFT WITH SPACE CHARGE

The equations of motion describing the longitudinal phase space evolution of particles accelerated in a synchrotron can be described by

$$\dot{\tau} = \frac{\eta}{\beta_s^2 E_s} w \qquad \dot{w} = \frac{q}{T_s} V(\tau),$$

where w describes the discrete energy gain, relative to that of the synchronous particle, about one turn. The revolution period of the synchronous particle is T_s and the slippage factor derived from the transverse optics is given by $\eta = 1/\gamma_t^2 - 1/\gamma^2$. Subscripted coordinates specify the synchronous particle.

Particles affected by a linear generalized voltage source $V(\tau)$ follow elliptical trajectories in longitudinal phase space described by the synchrotron frequency

$$\Omega^2 = -\frac{\eta}{\beta_s^2 E_s} \frac{q}{T_s} V'(\tau), \qquad (4)$$

where $V'(\tau) = \frac{d}{d\tau} V(\tau)$. In the case of a sinusoidal RF waveform given by peak voltage V_g, particles will experience a voltage gradient describable by

$$V'_{RF}(\tau) = h\omega_s V_g \cos\varphi,$$

where φ is the RF phase such that $\varphi = h\omega_s(\tau + t_s)$ where h is RF harmonic and ω_s is the angular revolution frequency of the synchronous particle. For particles oscillating in the center of the bunch with small phase space amplitudes ($\varphi \approx \varphi_s$), the synchronous synchrotron frequency is defined by

$$\Omega_s^2 = -\frac{\eta}{\beta_s^2 E_s}\frac{qV_g}{T_s}h\omega_s \cos\varphi_s.$$

In a non-accelerating bucket, particles with larger oscillation amplitudes $\hat{\phi} = h\omega_s\hat{\tau}$ will experience a nonlinear RF gradient and accordingly the normalized synchrotron tune μ is given by

$$\mu = \Omega/\Omega_s = \frac{\pi}{2K(\sin\hat{\phi}/2)} \approx 1 - \frac{\hat{\phi}^2}{16} + \mathcal{O}(\hat{\phi}^4),$$

where $K(m)$ is the complete elliptic integral of the first kind. The net effect of this tune spread is that particles at larger oscillation amplitudes will lag behind the synchrotron particle in terms of (τ, w) longitudinal phase space at varying rates. Accordingly, a bunch whose phase space distribution widths (σ_τ and σ_w) are not matched, will filament and expand as illustrated in Fig. 5.
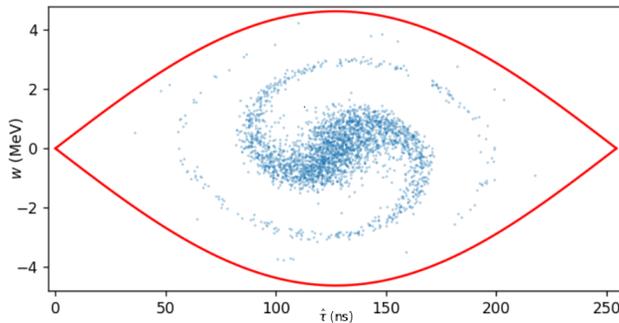

Figure 5: Filamentation due to tune spread of single-particle motion within a separatrix (red) indicating stable motion.

This filamentation induces bunch length oscillations that continue until eventually reaching an equilibrium. The synchrotron frequency spread also contributes as a stabilizing mechanism against longitudinal perturbations through Landau damping.

The effects of space charge induced voltage and RF voltage kicks can be combined such that the net voltage gradient is given by $V'(\tau) = V'_{RF}(\tau) + V'_{SC}(\tau)$ and

$$V'_{SC}(\tau) = \frac{g}{\omega_s}\frac{Z_0}{\beta_s\gamma_s^2}\frac{d^2\lambda}{d\tau^2}.$$

As the synchrotron frequency scales according to $\Omega^2 \propto V'(\tau)$, the normalized space charges tune shift is given by

$$\mu = \sqrt{1 + \frac{V'_{SC}}{V'_{RF}}}. \tag{5}$$

In the case of a Gaussian longitudinal bunch profile, the space charge tune shift is most significant for small oscillation amplitudes where the space charge gradient is the highest.

TRANSVERSE EFFECTS

Particles tracked through transverse optics described by beta function $\beta(s)$ and dispersion function $D(s)$, will follow trajectories given by

$$u(s) = \sqrt{\beta(s)\epsilon}\cos(\mu(s) + \mu_0) + D(s)\delta$$

where $u(s)$ is the particle's transverse offset at longitudinal position s, ϵ is a single particle's transverse emittance, the momentum spread is given by $\delta = (p - p_s)/p_s$, and the betatron phase advance is given by

$$\mu(s) = \int_0^s \frac{ds'}{\beta(s')}.$$

For a matched distribution, the statistical beam width along the ring is given by

$$\sigma_u^2(s) = \beta(s)\sigma_\epsilon + D(s)^2\sigma_\delta^2$$

where σ_δ and σ_ϵ describe the transverse bunch RMS momentum spread and emittance respectively.

The transverse optics of the PS (Fig. 6) are quasi-periodic and can be succinctly described by the Fourier series

$$\beta(\theta) \approx \sum_k \beta_k e^{ik\theta} \quad \text{and} \quad D(\theta) \approx \sum_k D_k e^{ik\theta}$$

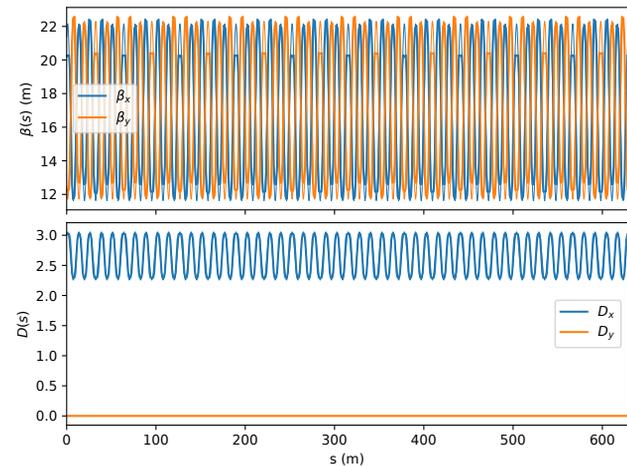whose primary coefficients are defined in Table 1.

Figure 6: PS transverse optics, expressible as Fourier sum.

Table 1: Main Fourier coefficients of PS optics

k	β_x	β_y	D_x	D_y
0	16.89	17.01	2.66	0
50	4.43-2.84i	-4.46+2.86i	0.34+0.22i	0

Approximating further that the beta and dispersion functions are constant throughout the PS such that $D(s) \approx D_0$ and $\beta(s) \approx \beta_0$, the effective transverse position for a particle, defined by properties $X \in \{\delta, \epsilon_x, \epsilon_y, \mu_x, \mu_y\}$, is given by

$$\overline{r^2}(X) = \overline{x^2} + \overline{y^2} \approx \frac{\beta_0}{2}(\epsilon_x + \epsilon_y) + D^2\delta^2.$$

MOP13

Because the betatron tune is typically high, the effects of transverse phase advance μ_x, μ_y will average out and can be largely neglected. Similarly, the effective beam size can be approximated by $a^2 = 4\sigma_x\sigma_y$, the geometric mean of horizontal and vertical beam size dimensions. Essentially constant throughout the ring, the beam size is given by properties $Y \in \{\sigma_\epsilon, \sigma_\delta\}$ such that

$$\bar{a}(Y) \approx 2\sqrt[4]{(\beta_0\sigma_\epsilon + D_0^2\sigma_\delta^2)(\beta_0\sigma_\epsilon)}.$$

The averaged geometry factor $\bar{g}$ for an arbitrary particle X within a uniform transverse distribution Y is therefore approximated by

$$\bar{g}(X, Y) \approx \frac{1}{2} + \ln\frac{b}{\bar{a}(Y)} - \frac{1}{2}\frac{\overline{r^2}(X)}{\bar{a}^2(Y)}.$$

Because $\bar{g} \propto -\overline{r^2}$ and $\overline{r^2} \propto \epsilon \propto \delta^2$, it can be shown that the nominal synchrotron tune shift described by Eq. (5), is reduced for particles whose transverse emittance or momentum spread is large.

The aforementioned relationships with the effective geometry factor $\bar{g}$, particle properties X, and beam properties Y were numerically verified by transverse tracking. Depicted in Fig. 7, a matched transverse distribution whose emittance is given by a Rayleigh distribution $\epsilon \sim R^2(\sqrt{\sigma_\epsilon})$, and uniformly distributed phase advance $\mu \sim U(-\pi, \pi)$, was tracked once through the PS ring with respect to the aperture radius b and beam width a.
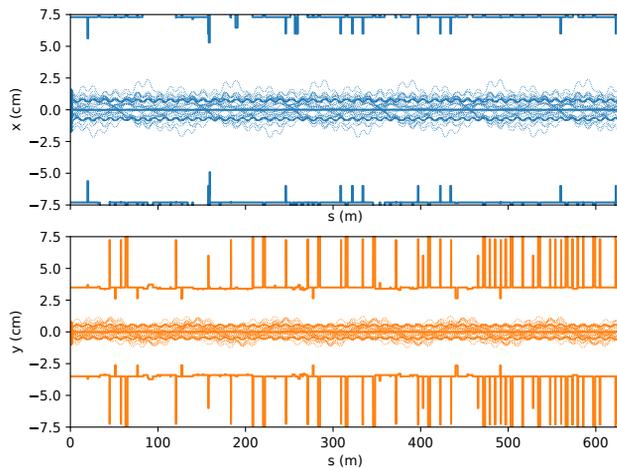
Figure 7: Horizontal (blue) and vertical (orange) trajectories for a matched transverse distribution are tracked through the PS aperture to compute each particle's incurred space charge geometry factor.

A meshed grid of particle properties X was tracked with respect to beam properties Y to generate a response matrix for $\bar{g} = \bar{g}(X, Y)$. Given Y, it was confirmed numerically that $\bar{g} \propto \delta^2$ (Fig. 8), that $\bar{g} \propto \epsilon$ (Fig. 9) where particle momentum spread is low, and that the dependence of $\bar{g}$ on transverse phase advance is broadly sinusoidal (Fig. 10).
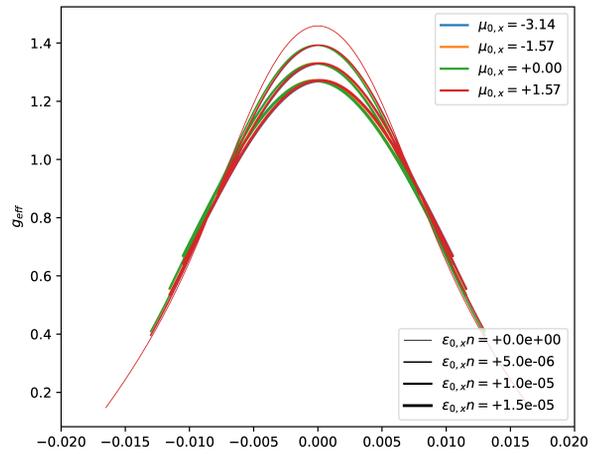
Figure 8: The effective geometry factor $\bar{g}$ scales with δ^2 and linearly with emittance ϵ_x (line thickness).
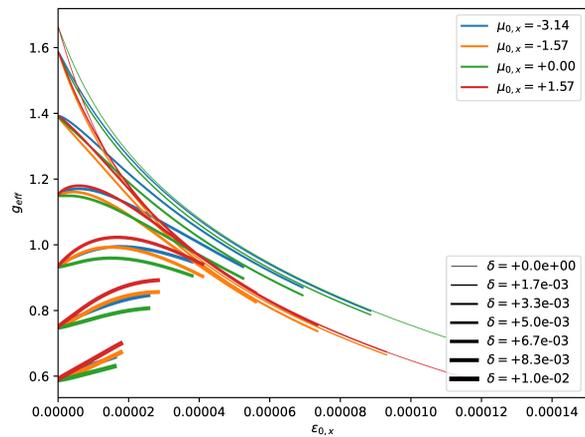
Figure 9: The geometry factor $\bar{g}$ scales linearly with emittance ϵ_x where momentum spread δ (line thickness) is low. The domain X is limited by the aperture radius b.
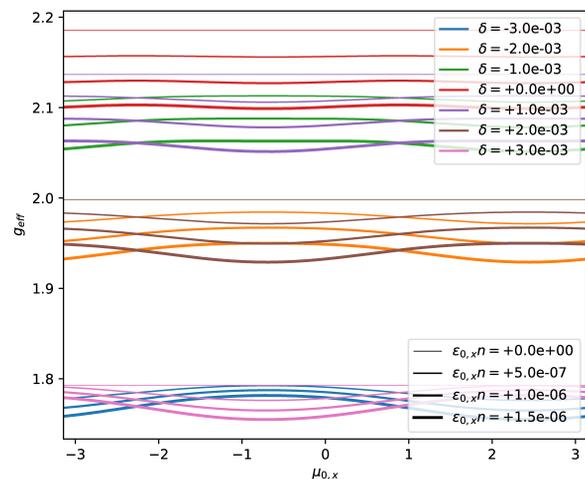
Figure 10: The geometry factor $\bar{g}$ is sinusoidally dependent on phase advance μ_x, however this is dominated by momentum spread δ (color) and transverse emittance ϵ_x (thickness).

SIMULATION RESULTS

The Beam Longitudinal Dynamics code (BLonD) has been developed at CERN to track the evolution of an ensemble of particles with intensity effects in synchrotrons [8]. By default, the code incorporates the effects of complex RF harmonic systems by means of RF energy kicks. Each turn, an RF gap of voltage V_g at harmonic h will discretely increment a particle's relative kinetic energy change w given by

$$w = qV(\tau) = q(V_{RF} + V_W), \quad (6)$$

where $V_{RF} = qV_g(\sin\varphi - \sin\varphi_s)$ and V_W is given by Eq. (3) where, in general, space charge can be combined with other impedance sources.

Of the particle properties X relevant for estimating the geometry factor $\bar{g}$, used in Eq. (6), momentum spread δ is evaluated once per turn. Because transverse emittance ϵ_x, ϵ_y is assumed to be preserved and phase advance deemed inconsequential, the particle properties follow that

$$X_i(\delta_i, \epsilon_x, \epsilon_y) \rightarrow X_{i+1}(\delta_{i+1}, \epsilon_x, \epsilon_y),$$

where i indicates the turn number. The tracked beam size $\bar{a}$, the momentum spread variance σ_δ^2 can also be evaluated once per turn such that

$$Y_i(\sigma_{\delta,i}, \sigma_\epsilon) \rightarrow Y_{i+1}(\sigma_{\delta,i+1}, \sigma_\epsilon).$$

The evolution of $\bar{g}_i(X_i, Y_i)$ required to derive V_W due to space charge was implemented in BLonD. Representative of the PS at flat bottom, a gaussian bunch of length $4\sigma_\tau = 120$ ns and transverse emittance $\sigma_\epsilon = 1 \times 10^{-6}$ was tracked against a 22 kV RF voltage source at harmonic 9. The bunch intensity was exaggerated at $N = 2 \times 10^{12}$ protons to better demonstrate intensity effects.

A particle's synchrotron frequency is computed by taking the FFT of it's tracked phase evolution over time. As depicted in Fig. 11, the nominal synchrotron frequency shift due to space charge is reduced by varying amounts when incorporating transverse motion through the effective geometry factor $\bar{g}$. This variance in synchrotron frequency of particles with similar oscillation amplitudes $\hat{\tau}$ could be described as a "blurring" of synchrotron frequency tune.
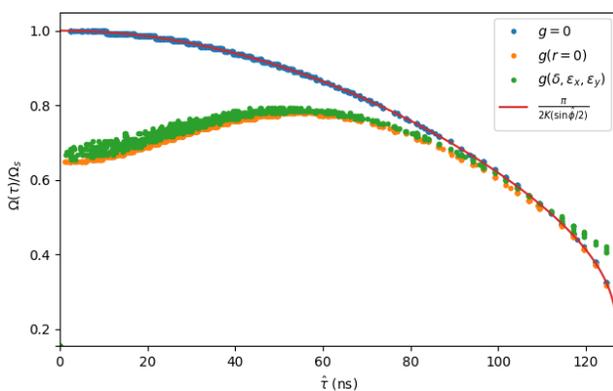
Figure 11: Tune spread (blue), shift (orange) and blur (green) for a long round beam with a uniform transverse distribution and Gaussian longitudinal profile.

In this example, particles tracked in longitudinal phase space will circulate around the bunch center at varying rates independent of oscillation amplitude. The phenomena of filamentation present due to synchrotron frequency spread is seen to be systematically increased and "blurred" when incorporating transverse effects (Fig. 12), suggesting an otherwise overlooked stabilizing phenomenon.
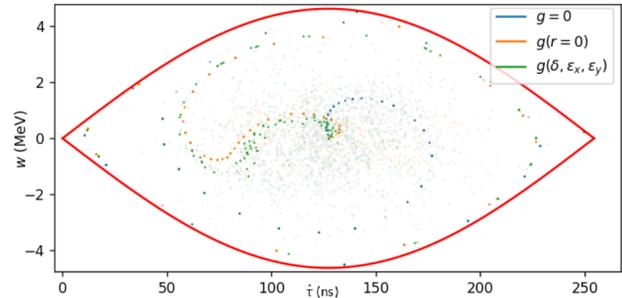
Figure 12: Selected particles, emphasized among a matched distribution, are shown to filament about the bucket center within the separatrix (red) due to tune spread (blue). The effect of space charge tune shift (orange) is observed to be "blurred" when incorporating transverse motion (green).

CONCLUSIONS

It has been demonstrated that particles at a given longitudinal position will experience varying levels of longitudinal space charge according to an individual particles transverse emittance and momentum spread. Particles with off-axis trajectories will experience less space charge, reducing the space charge tune shift or conversely, increasing the synchrotron frequency. This observed spread in synchrotron frequency may further increase the bulk longitudinal filamentation rate, normally produced by the non-linearities of an accelerating RF voltage alone, which could also contribute to overall beam stability.

Further work might involve designing bunch length oscillation experiments to observe variations in the synchrotron frequency [10] as a function of the transverse beam parameters. Additionally, the description of the effective geometry factor could be further refined by incorporating elliptical geometries, more closely approximating that of the real PS aperture.

ACKNOWLEDGMENTS

REFERENCES

[1] S. Y. Lee, *Accelerator physics 2nd ed.*, Singapore: World Scientific, 2004.

[2] M. Ferrario, M. Migliorati, and L. Palumbo, "Space charge effects," CERN, Geneva, Switzerland, CERN-2014-009, pp. 331-356, 2013. doi:10.5170/CERN-2014-009.331

[3] H. Damerau, A. Lasheen, and M. Migliorati, "Observation and damping of longitudinal coupled-bunch oscillations in the CERN PS," presented at the ICFA Mini-Workshop "Impedances and Beam Instabilities in Particle Accelerators", 2018, p. 33. doi:10.23732/CYRCP-2018-001.33

[4] M. Migliorati, S. Persichelli, H. Damerau, S. Gilardoni, S. Hancock, and L. Palumbo, "Beam-wall interaction in the CERN Proton Synchrotron for the LHC upgrade," *Phys. Rev. ST Accel. Beams*, vol. 16, p. 031001, 2013. doi:10.1103/PhysRevSTAB.16.031001

[5] H. Damerau, A. Funken, R. Garoby, S. Gilardoni, B. Goddard, K. Hanke, A. Lombardi, D. Manglunki, M. Meddahi, B. Mikulec, G. Rumolo, E. Shaposhnikova, M. Vretenar, and J. Coupard, "LHC Injectors Upgrade, Technical Design Report," CERN, Geneva, Switzerland, Tech. Rep. CERN-ACC-2014-0337, 2014. https://cds.cern.ch/record/1976692

[6] J. Coupard, H. Damerau, A. Funken, R. Garoby, S. Gilardoni, B. Goddard, K. Hanke, D. Manglunki, M. Meddahi, G. Rumolo, R. Scrivens, and E. Chapochnikova, "LHC Injectors Upgrade, Technical Design Report," CERN, Geneva, Switzerland, Tech. Rep. CERN-ACC-2016-0041, 2016. https://cds.cern.ch/record/2153863

[7] O. Aberle *et al.,* "High-Luminosity Large Hadron Collider (HL-LHC): Technical design report", CERN Yellow Reports: Monographs, CERN, Geneva, Switzerland, CERN-2020-010, 2020. https://cds.cern.ch/record/2749422

[8] "CERN beam longitudinal dynamics code BLonD," https://blond.web.cern.ch/.

[9] A. Lasheen, H. Damerau, A. Huschauer, and B. K. Popovic, "Longitudinal Microwave Instability Study at Transition Crossing with Ion Beams in the CERN PS", in *Proc. 12th Int. Particle Accelerator Conf. (IPAC'21)*, Campinas, Brazil, May 2021, pp. 3197–3200. doi:10.18429/JACoW-IPAC2021-WEPAB243

[10] A. Lasheen, "Longitudinal space charge in the SPS," CERN, Geneva, Switzerland, Tech. Rep. CERN-ACC-NOTE-2016-0074, 2016. https://cds.cern.ch/record/2238995